Chinese Journal of Chemistry, **2009**, *27*, 1925—1928

Full Paper

Preparation of Polyelectrolyte Nanotubes by a Pressure-filter-template Technique Using Microporous Anodic Aluminum Oxide (AAO) as the Template

MENG, Xiuxia*(孟秀霞) YANG, Naitao(杨乃涛) TAN, Xiaoyao(谭小耀)

School of Chemical Engineering, Shandong University of Technology, Zibo, Shandong 255049, China

Polyelectrolyte nanotubes of poly(sodium 4-styrene-sulfonate) (PSS) with cationic poly(diallyl dimethyl ammonium chloride) (PDDA) (PSS/PDDA) were fabricated by a pressure-filter-template technique using microporous anodic aluminum oxide (AAO) as the template. UV-Vis spectroscopy, scanning electron microscopy (SEM), transmission electron microscopy (TEM), X-ray diffraction (XRD) and infrared spectroscopy (FT-IR) were applied to characterize the obtained PSS/PDDA nanotubes. The results have shown that the PSS/PDDA nanotubes exhibit an amorphous structure and have the outer diameter of 200 nm and length of 25 μm respectively, which are in good agreement with the dimensions of the AAO template pores. The wall thickness of the nanotubes may be controlled by the number of the self-assembled layers. Formation of the nanotubes follows a layer-by-layer (LbL) mechanism due to the electrostatic interactions, where the SO_3^- groups of PSS are first adsorbed on the Lewis acid sites of AAO template pores.

Keywords polyelectrolyte, nanotube, anodic aluminum oxide, template, layer-by-layer assembly

Introduction

In the last decade, considerable efforts have been focused on the fabrication of one-dimensional (1D) nanomaterials such as nanotubes, nanowires or nanorods due to their novel properties and the potential applications to optics, electronics, catalysts, sensors, *etc*.[1-5] Nanotubes may be formed from a variety of materials including carbon, ceramics, metals and organic polymers.[6-9] The organic polymer nanotubes possess high resistance to chemical and structural imperfection and nice ability to form ordered films, and thus have attracted increasing interests in recent years.[10-14]

The template method has been widely used for the preparation of 1D nanomaterials due to its simplicity and versatility in operations. It can be generally assorted into two categories: the solution immersion technique, which is usually applied to non-aqueous systems and the pressure-filter-template technique, which is suitable for aqueous systems.[15-20] Amongst a majority of templates, anodic porous alumina oxide (AAO) membrane which is fabricated by the anodic oxidation of aluminum in an acidic electrolyte is the most popular one because of its distinct advantages such as the low cost, controllable pore diameter, narrow pore size distribution and the high chemical and thermal stability.[21-27]

The polyelectrolyte complex of anionic poly(sodium 4-styrene-sulfonate) (PSS) with cationic poly(diallyl dimethyl ammonium chloride) (PDDA) has found extensive applications to electrochemistry,[12] biotechnology[28] and as a piezoelectric material.[29] For example, the PSS/PDDA nanotubes may be used to modify electrode so that the electrode will possess a wide linear range and an excellent stability. In this work, PSS/PDDA nanotubes were obtained via a pressure-filter-template technique using AAO as the template.

Experimental

Fabrication of PSS/PDDA nanotubes

Anionic poly(sodium 4-styrene-sulfonate) (PSS, M_w 70000) and cationic poly(diallyl dimethyl ammonium chloride) (PDDA, 20% (*w*), M_w 400000—500000) (both from Sigma-Aldrich Co Ltd) were dissolved respectively in deionized water to form aqueous solutions of 1 mg/mL. Microporous anodic aluminum oxide membranes (AAO, from Whatman Corp.) having Φ 25 mm diameter, 25 μm thickness and average pore diameter of 0.2 μm were ultrasonically cleaned in alcohol to remove the residues on surfaces. The cleaned AAO templates were placed on a sand core funnel filter plate and then dipped alternately into the PSS and PDDA aqueous solutions for 2 h under a vacuum, −0.05 MPa. This dipping process was repeated in a cyclic mode. After each depositing operation, the template was polished carefully with fine grit sandpaper and washed with distilled water to remove the polyelectrolyte residues on the template surfaces. After drying in a vacuum box, the

* E-mail: mengxiux@sdut.edu.cn; Tel.: 0086-533-2786292; Fax: 0086-533-2786292
Received December 16, 2008; revised May 6, 2009; accepted June 1, 2009.
Project supported by the National Natural Science Foundation of China (No. 20676073).

© 2009 SIOC, CAS, Shanghai, & WILEY-VCH Verlag GmbH & Co. KGaA, Weinheim

deposited AAO templates were dissolved partly in a 6 mol/L NaOH aqueous solution. Three successive centrifugal separations followed by washing with pure water were performed to obtain PSS/PDDA nanotubes.

Characterization

The process of multilayer self-assembly was monitored by means of UV-Vis spectroscopy (Lambda 35 spectrophotometer, American). The morphology and dimension of the PSS/PDDA nanotubes were measured by scanning electron microscopy (SEM, FEI Sirion-200, the Netherlands). Transmission electron microscopy (TEM) images were obtained with a Hitech-800 microscope. The samples for TEM were ultrasonicated before the measurements. X-ray diffraction (XRD) patterns of the nanotubes were recorded using a diffractometer (Bruker D8 Advance, Germany) with Cu-Kα radiation (λ=0.15404 nm). A continuous scan mode was used to collect 2θ data from 3° to 50° with a 0.02° sampling pitch and a 2(°)•min^{-1} scanning rate. The X-ray tube voltage and current were set at 40 kV and 30 mA, respectively. To investigate the assembly structure of PSS on the AAO template, the first layer of films was analyzed by infrared spectroscopy (FT-IR) using a Nicolet 5700 instrument (KBr pressed pellet method).

Results and discussion

Figure 1 shows the UV-Vis spectra of the PSS/PDDA nanotubes with respect to the different deposited layers. As can be seen, there are two strong absorption peaks present on the UV-Vis plot at around 195 and 225 nm, which increase with the number of the deposited layer. This indicates that the PSS and the PDDA molecules have been successfully assembled onto the pore walls of the AAO template. As shown in Figure 2 where the molecular structures of PSS and PDDA are presented, the phenyl group in PSS may transfer from $\pi \rightarrow \pi^*$ under UV-Vis, leading to the absorption at 195 and 225 nm wavelength. Meanwhile, the n-σ^* transition of N atom in the pyrrole ring of PDDA molecules gives an absorption at 220 nm under UV-Vis, which is close to the absorption peak of PSS. As a result, the maximum absorptions on the UV-Vis patterns appear at 195 and 225 nm, indicating the presence of the PSS and PDDA molecules. On the other hand, the absorbance at 195 and 225 nm increases linearly with the number of the deposited layers, as shown in the inset of Figure 1. This implies that the assembly of the PSS/PDDA nanotubes follows the layer-by-layer (LbL) mechanism.[30] The more the assembled layers, the larger the thickness of the nanotubes, and thus the stronger the absorbance on the UV-Vis patterns.

Figure 3 shows the SEM micrographs of the PSS/PDDA nanotubes taken from the suspended floc after the AAO template was partly dissolved in a 6 mol/L NaOH solution. It can be seen that the PSS/PDDA nanotubes are very flexible and are arrayed

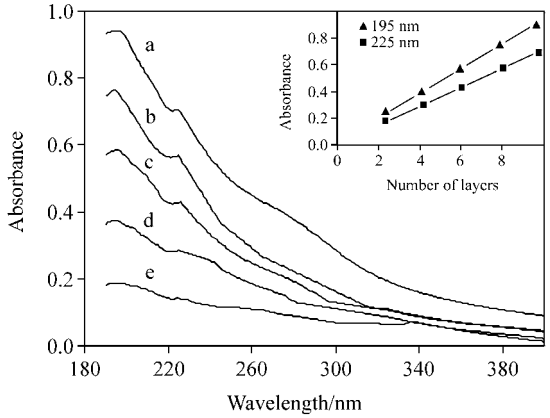

Figure 1 UV-Vis spectra of the PSS/PDDA nanotubes with (a) 10, (b) 8, (c) 6, (d) 4, and (e) 2 assembled layers. Inset: absorbance at 195 and 225 nm vs. assembled layers.

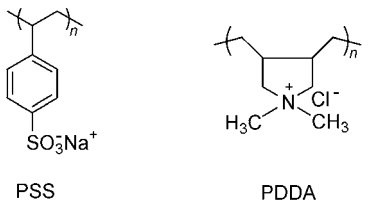

Figure 2 Structural formulas of the PSS and the PDDA molecules.

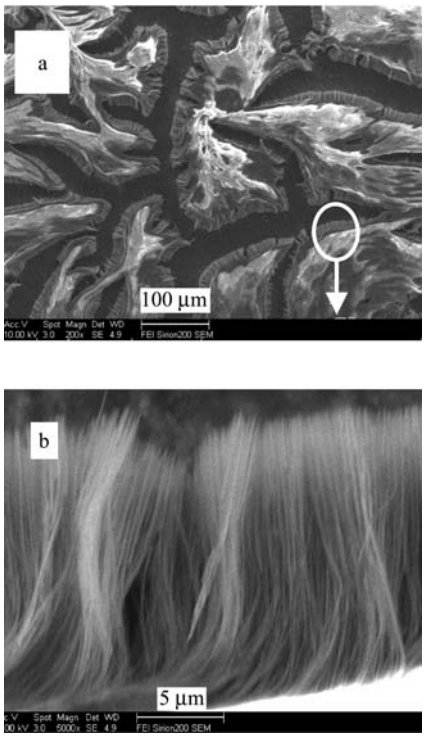

Figure 3 SEM images of the nonotubes. (a) PSS/PDDA nonotubes arrays in a large area, and (b) the image of a cluster of PSS/PDDA nonoatubes.

in a highly ordered mode on the residual template matrix. Since the AAO templates have a narrow pore size distribution, the PSS/PDDA nanotubes formed in the template pores possess a fairly uniform diameter. In

© 2009 SIOC, CAS, Shanghai, & WILEY-VCH Verlag GmbH & Co. KGaA, Weinheim

addition, the typical length of the nanotubes obtained from the figure is about 25 μm, which is in good agreement with the thickness of the AAO template. It suggests that the PSS and PDDA solutions have penetrated into the whole length of the AAO pores due to the filtration force. Therefore, the structure and the dimensions of the formed nanotubes may be controllable through selecting suitable templates with different structures.

In order to further investigate the morphology and the microstructure of the obtained PSS/PDDA nanotubes, TEM image was taken on the samples with four deposited layers, as shown in Figure 4. It can be seen clearly that the outer diameter of the nanotubes is close to the pore diameter of the AAO templates, 200 nm. In addition, the hollow nanostructure with internal separation can also be seen from the figure. This indicates that four assembled layers are not enough to fill the template pores to form nanorods.

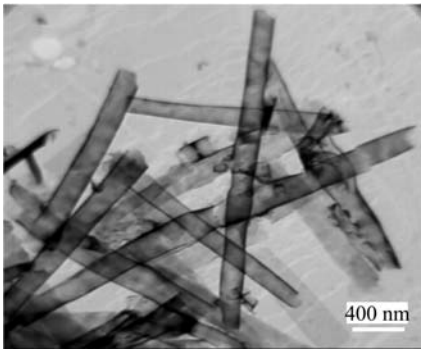

Figure 4 TEM images of the PSS/PDDA nonatubes with four deposited layers.

Figure 5 shows the X-ray diffraction (XRD) patterns of the PSS powders as well as the PSS/PDDA nanotubes. The convex peak in 20°—40° was attributed to the amorphous AAO template. It can be seen that the PSS powder shows some crystal characteristics, but the PSS/PDDA nanotube exhibits an amorphous structure. Therefore, the crystallinity of PSS actually has been eliminated after it is combined into the nanotubes, which may result from the orderliness of the self-assembled films.

Figure 6 shows the infrared spectrum of the PSS, AAO template and the first PSS layer absorbed on the AAO template. In Figure 6b, the absorption bands occurring at 1200 and 1130 cm^{-1} correspond to the Ar—H bending vibration. The bands at 1040 and 837 cm^{-1} were assigned to stretching vibration and bending vibration of S=O, respectively. Correspondingly, both bands shift to 1030 and 822 cm^{-1} (Figure 6c) due to the assembly of PSS on the AAO template pores. The absorption bands in the range of 650—900 cm^{-1} are the characteristic region of the substitution pattern on the aromatic ring. These phenomena suggest that PSS be adsorbed mainly by the sulfonic acid group on the Lewis acid site of the AAO template pore wall.[31]

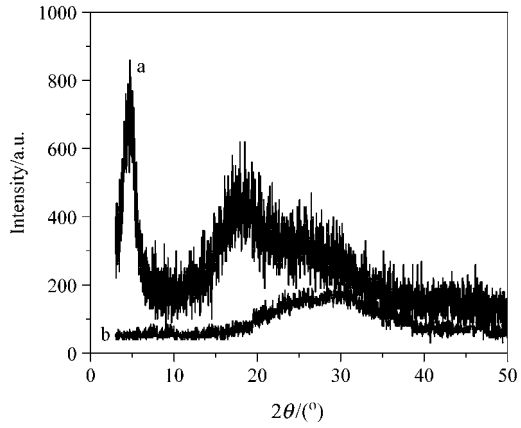

Figure 5 X-ray diffraction patterns of (a) PSS powder and (b) PSS/PDDA nanotubes.

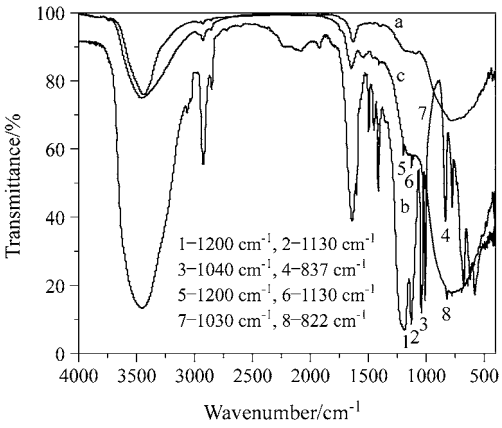

Figure 6 FT-IR spectra of (a) AAO template, (b) PSS and (c) first PSS layer absorbed on the AAO template.

The formation mechanism of the PSS/PDDA nanotubes may be illustrated in Figure 7. The negatively charged PSS molecules are first adsorbed and nucleated preferentially on the positively charged walls of the AAO template pores by the electrostatic interaction.[32,33] The cationic sites can also be viewed as "molecular anchors" which guide the PSS molecules depositing on the pore walls. The PDDA with positive charges are then absorbed on the PSS because of electrostatic interaction. According to this mechanism, PSS and PDDA are deposited alternately on the pore walls of AAO template. Therefore, the PSS/PDDA nanotubes with different thicknesses can be obtained by controlling the number of assembled layers. It should be mentioned that other macromolecular polyelectrolyte nanotubes with opposite charges can also be prepared by the pressure-filter-template technique using porous anodic alumina oxide as template.

Conclusion

Flexible, uniform and highly ordered PSS/PDDA nanotubes have been successfully synthesized by the pressure-filter-template technique using porous anodic

© 2009 SIOC, CAS, Shanghai, & WILEY-VCH Verlag GmbH & Co. KGaA, Weinheim

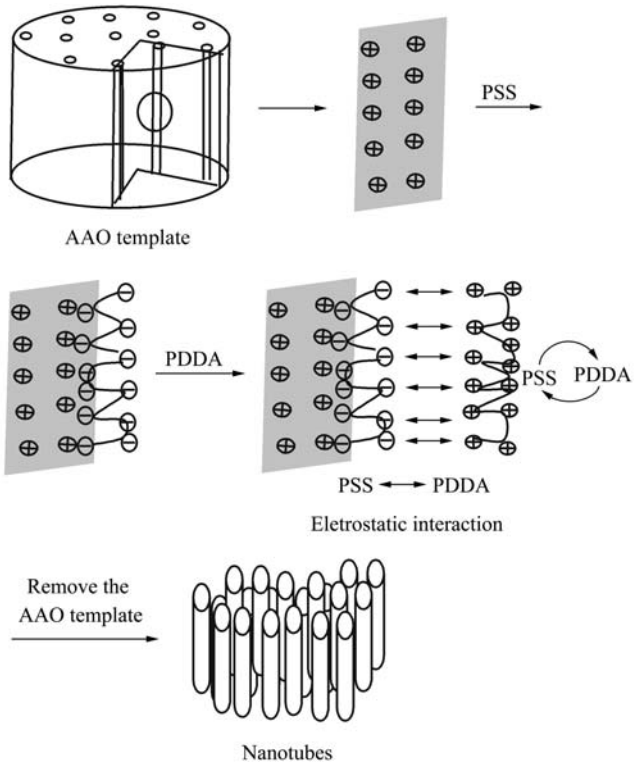

Figure 7 Schematic presentation of the formation of PSS/PDDA nanotubes by self-assembly on template.

alumina oxide as the template. The resultant nanotubes exhibit non-crystalline phase due to the orderliness of self-assembled films, and have an outer diameter of 200 nm and a length of 25 μm, which are in good agreement with the dimension of the template pores. The assembly of PSS/PDDA nanotubes follows the layer-by-layer (LbL) mechanism, where the SO_3^- groups in PSS are first adsorbed on the Lewis acid sites of AAO pores and then PDDA with positive charges are assembled on the PSS by electrostatic interaction. PSS and PDDA can be deposited alternately. Thus the wall thickness of the nanotubes may be controlled by the number of the self-assembled layers.

References

1 Panda, A. B.; Glaspell, G.; El-Shall, M. S. *J. Phys. Chem. C* **2007**, *111*, 1861.
2 Ding, S.; Xu, J.; Chen, H. *Chem. Commun*. **2006**, *34*, 3631.
3 Yu, D.; Qian, J.; Xue, N.; Zhang, D.; Wang, C.; Guo, X.; Ding, W.; Chen, Y. *Langmuir* **2007**, *23*, 382.
4 Sun, Z.; Yuan, H.; Liu, Z.; Han, B.; Zhang, X. *Adv. Mater*. **2005**, *17*, 2993.
5 Zhang, W.; Cui, X. L.; Jiang, Z. Y. *Acta Chim. Sinica* **2008**, *66*, 867 (in Chinese).
6 Hu, J. T.; Odom, T. W.; Lieber, C. M. *Acc. Chem. Res*. **1999**, *32*, 435.
7 Edelmann, F. T. *Angew. Chem., Int. Ed*. **1999**, *38*, 1381.
8 Mitchell, D. T.; Lee, S. B.; Trofin, L.; Li, N. C.; Nevanen, T. K.; Soderlund, H.; Martin, C. R. *J. Am. Chem. Soc*. **2002**, *124*, 11864.
9 Klefenz, H. *Eng. Life Sci*. **2004**, *4*, 211.
10 Decher, G.; Hong, J. D. *Makromol. Chem., Macromol. Symp*. **1991**, *46*, 321.
11 Decher, G. *Science* **1997**, *277*, 1232.
12 Qian, L.; Liu, Y.; Song, Y.; Li, Z.; Yang, X. *Electrochem. Commun*. **2005**, *7*(12), 1209.
13 Yang, Y.; He, Q.; Duan, L.; Cui, Y.; Li, J. B. *Biomaterials* **2007**, *28*, 3083.
14 Wang, Y. T.; Wang, H.; Cheng, C.; Chen, S.; Kan, S.; Chen, C.; Hu, J.; Su, Z. *Chin. J. Chem*. **2007**, *25*, 1090.
15 Zelenski, C. M.; Dorhout, P. K. *J. Am. Chem. Soc*. **1998**, *120*, 734.
16 Gong, G. J.; She, X. L.; Fu, Z. F.; Li, J. J. *J. Mater. Res*. **2004**, *19*, 3324.
17 Ai, S.; Cui, Y.; He, Q.; Tao, C.; Li, J. B. *Colloids Surf., A* **2006**, *275*, 218.
18 Ai, S. F.; Lu, G.; He, Q.; Li, J. B. *J. Am. Chem. Soc*. **2003**, *125*, 11140.
19 Ai, S. F.; He, Q.; Tao, C.; Zheng, S. P.; Li, J. B. *Macromol. Rapid Commun*. **2005**, *26*, 1965.
20 Tian, Y.; He, Q.; Cui, Y.; Tao, C.; Li, J. B. *Chem. Eur. J*. **2006**, *12*, 4808.
21 Chen, J.; Tao, Z. L.; Li, S. L. *J. Am. Chem. Soc*. **2004**, *126*, 3060.
22 Cao, H. Q.; Xu, Y.; Hong, J. M.; Liu, H. B.; Yin, G.; Li, B. L.; Tie, C. Y.; Xu, Z. *Adv. Mater*. **2001**, *13*, 1393.
23 Steinhart, M.; Wendorff, J. H.; Greiner, A.; Wehrspohn, R. B.; Nielsch, K.; Schilling, J.; Choi, J.; Gösele, U. *Science* **2002**, *296*, 1997.
24 Steinhart, M.; Wehrspohn, R. B.; Gösele, U.; Wendorff, J. H. *Angew. Chem., Int. Ed*. **2004**, *43*, 1334.
25 Steinhart, M.; Wehrspohn, R. B.; Wendorff, J. H. *Chem. Phys. Chem*. **2003**, *4*, 1171.
26 Steinhart, M.; Jia, Z.; Schaper, A.; Wehrsphon, R. B.; Gösele, U.; Wendorff, J. H. *Adv. Mater*. **2003**, *15*, 706.
27 Liu, H. B.; Li, Y. L.; Lei, J.; Luo, H. Y.; Xiao, S. Q.; Fang, H. J.; Li, H. M.; Zhu, D. B.; Yu, D. P.; Xu, J.; Xiang, B. *J. Am. Chem. Soc*. **2002**, *124*, 13370.
28 Forrest, S. R.; Elmore, B. B.; Palmer, J. D. *Appl. Biochem. Biotechnol*. **2005**, *121*(1—3), 85.
29 Zeng, Z.; Claus, R.; Liu, Y.; Zhang, F.; Du, W.; Cooper, K. L. *Smart Mater. Struct*. **2000**, *9*, 801.
30 Tang, J.; Li, W. J.; Wang, Y.; Wang, B.; Sun, J.; Yang, B. *J. Photochem. Photobiol., A* **2001**, *141*, 179.
31 Li, N. C.; Martin, C. R. *J. Electrochem. Soc*. **2001**, *148*(2), A164.
32 Martin, C. R. *Science* **1994**, *266*, 1961.
33 Pouget, P.; Jozefowica, M. E.; Epstein, A. J.; Tang, X.; MacDiarmid, A. G. *Macromolecules* **1991**, *24*, 779.

(E0812161 Li, L.; Fan, Y.)

© 2009 SIOC, CAS, Shanghai, & WILEY-VCH Verlag GmbH & Co. KGaA, Weinheim